REPORT DOCUMENTATION PAGE

Public reporting burden for this collection of information is estimated to average 1 hour per response, including the time for reviewing instructions, searching existing data sources, gathering and maintaining the data needed, and completing and reviewing this collection of information. Send comments regarding this burden estimate or any other aspect of this collection of information, including suggestions for reducing this burden to Department of Defense, Washington Headquarters Services, Directorate for Information Operations and Reports (0704-0188), 1215 Jefferson Davis Highway, Suite 1204, Arlington, VA 22202-4302. Respondents should be aware that notwithstanding any other provision of law, no person shall be subject to any penalty for failing to comply with a collection of information if it does not display a currently valid OMB control number. **PLEASE DO NOT RETURN YOUR FORM TO THE ABOVE ADDRESS.**

1. REPORT DATE (DD-MM-YYYY)	2. REPORT TYPE	3. DATES COVERED (From - To)
01-03-2010	Technical Paper	

4. TITLE AND SUBTITLE

Reactions Leading to Ignition in Nanocomposite Al-oxide Systems

5a. CONTRACT NUMBER
FA9300-08-C-2103

5b. GRANT NUMBER

5c. PROGRAM ELEMENT NUMBER

6. AUTHOR(S)

Alexandre Ermoline, Mirko Schoenitz (Reactive Metals, Inc.); Edward L. Dreizin

(New Jersey Institute of Technology)

5d. PROJECT NUMBER

5e. TASK NUMBER

5f. WORK UNIT NUMBER
OSDBR8WD

7. PERFORMING ORGANIZATION NAME(S) AND ADDRESS(ES)

Air Force Research Laboratory (AFMC)
AFRL/RZSP
10 E. Saturn Blvd.
Edwards AFB CA 93524-7680

8. PERFORMING ORGANIZATION REPORT NUMBER

AFRL-RZ-ED-TP-2010-067

9. SPONSORING / MONITORING AGENCY NAME(S) AND ADDRESS(ES)

Air Force Research Laboratory (AFMC)

AFRL/RZS
5 Pollux Drive
Edwards AFB CA 93524-70448

10. SPONSOR/MONITOR'S ACRONYM(S)

11. SPONSOR/MONITOR'S NUMBER(S)
AFRL-RZ-ED-TP-2010-067

12. DISTRIBUTION / AVAILABILITY STATEMENT

Approved for public release; distribution unlimited (PA #10114).

13. SUPPLEMENTARY NOTES
For presentation at the 2010 Central State Section of the Combustion Institute, Champaign, IL, 21-23 March 2010.

14. ABSTRACT

Aluminum-metal oxide energetic compositions with components mixed on the nano-scale are substantially more reactive than conventional thermites and are of interest as potential additives to propellants, explosives, and pyrotechnics. For such nanocomposite materials prepared by Arrested Reactive Milling, the exothermic reactions leading to ignition were detected to begin at relatively low temperatures. These materials are prepared by mechanical processing at room temperature, and the nature of the interface present between aluminum and the oxidizer (metal oxide, e.g., CuO, MoO_3, Bi_2O_3, etc.) is unknown. Initial estimates show that the reaction rates observed in thermo-analytical experiments cannot be explained assuming that the metal and oxidizer are separated by a substantial oxide layer, similar to that present on the surface of conventional aluminum particles. Experiments using a Thermal Activity Monitor (TAM III) quantify the reaction rates between aluminum and oxidizer at temperatures as low as 30 °C; the results of these measurements are presented and discussed in the context of the redox reactions leading to ignition in such materials.

15. SUBJECT TERMS

16. SECURITY CLASSIFICATION OF:			17. LIMITATION OF ABSTRACT	18. NUMBER OF PAGES	19a. NAME OF RESPONSIBLE PERSON Mr. Milton McKay
a. REPORT	b. ABSTRACT	c. THIS PAGE	SAR	9	19b. TELEPHONE NUMBER (include area code) N/A
Unclassified	Unclassified	Unclassified			

Reactions leading to ignition in nanocomposite Al-oxide systems

Alexandre Ermoline[1], Mirko Schoenitz[1], Edward L. Dreizin[2*]
[1]Reactive Metals, Inc., Newark, NJ 0102
[2]New Jersey Institute of Technology, Newark, NJ 07102

Abstract
Aluminum-metal oxide energetic compositions with components mixed on the nano-scale are substantially more reactive than conventional thermites and are of interest as potential additives to propellants, explosives, and pyrotechnics. For such nanocomposite materials prepared by Arrested Reactive Milling, the exothermic reactions leading to ignition were detected to begin at relatively low temperatures. These materials are prepared by mechanical processing at room temperature, and the nature of the interface present between aluminum and the oxidizer (metal oxide, e.g., CuO, MoO_3, Bi_2O_3, etc.) is unknown. Initial estimates show that the reaction rates observed in thermo-analytical experiments cannot be explained assuming that the metal and oxidizer are separated by a substantial oxide layer, similar to that present on the surface of conventional aluminum particles. Experiments using a Thermal Activity Monitor (TAM III) quantify the reaction rates between aluminum and oxidizer at temperatures as low as 30 ºC; the results of these measurements are presented and discussed in the context of the redox reactions leading to ignition in such materials.

Introduction

Multiple reactive compositions include aluminum powders or nanopowders, e.g., [1 – 3]. Aluminum particles can be mixed with various oxidizers, including ammonium perchlorate, metal oxides, and other compounds. In all such mixtures, the initial reactions leading to aluminum ignition are rate limited by relatively slow diffusion of the reacting species through the protective natural aluminum oxide layer always present on the Al surface exposed to air [4 – 7]. However, the reactive interfaces existing in nanocomposite materials prepared by Arrested Reactive Milling (ARM) [8] are not exposed to gaseous oxidizer during the material preparation. Indeed, during the mechanical milling performed under inert environment, when a fresh aluminum surface is produced, it is immediately pressed against that of the solid oxidizer particles, e.g., CuO, MoO_3, etc. As a result, fully dense, nanocomposite structures are formed, as that shown in Fig. 1. It is unclear whether a passivating Al_2O_3 layer, similar to that present on any aluminum surface exposed to air, also exists between inclusions or layers of metallic Al and solid oxidizer fully consolidated within each powder particle prepared by ARM. If such an oxide layer is present, the kinetics of the initial exothermic reactions leading to ignition are expected to be similar to those in the composite materials comprising blends of aluminum powders with respective oxidizers. However, if the alumina layer is not formed, or if the structure and morphology of the layer separating metallic aluminum and oxidizer are different from those of amorphous alumina, it is reasonable to expect that the ignition kinetics for ARM-prepared materials are qualitatively different from those of the mixed powders or nanopowders with the same bulk composition. The objective of this effort is to establish whether initial exothermic reactions in the ARM-prepared nanocomposite thermites can be described using a conventional, thermally activated diffusion or whether a different reaction mechanism should be introduced.
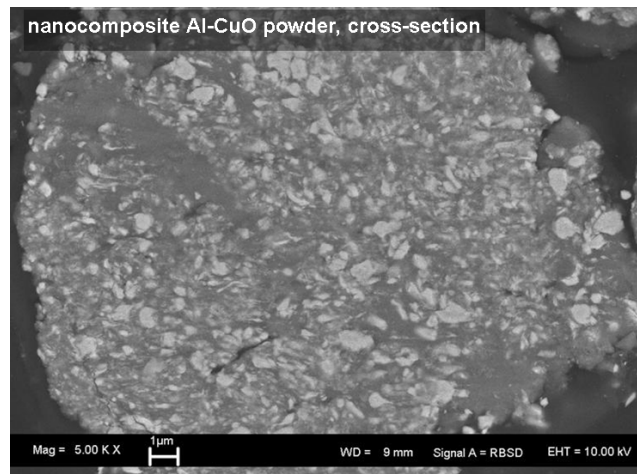

Fig. 1. A cross-sectioned particle of a nanocomposite Al-CuO material. Light-colored CuO inclusions are embedded into a dark-colored aluminum matrix.

Onset temperatures for the exothermic reactions in thermite compositions

Multiple literature reports are available on onset temperatures and reaction kinetics for exothermic reactions in thermite-type composite and nanocomposite materials prepared by mixing of nanopowders and by layered deposition of nanofoils. The deposition is performed at elevated temperatures that support a more extended reaction between the deposited layers.

For variety of aluminum based thermites, including Al-MoO$_3$ [9], Al-Fe$_2$O$_3$ [10], Al-I$_2$O$_5$ [11] and other systems, the onset of exothermic redox reactions was detected between 500 and 600 ºC, with lower temperatures observed for finer powders and nanopowders. Similarly, the onset of exothermic reactions in the same temperature range was observed for Al-CuO nanofoils [12, 13]. Note that this temperature range effectively coincides with the temperatures at which the first oxidation step for aluminum powders and nanopowders is observed in gaseous oxidizers [4 – 7].

Detailed studies of exothermic reactions in the ARM-prepared nanocomposite thermites [14 – 17] showed that the reaction onset is observed at a much lower temperatures, between 150 and 250 ºC. This significant difference in the onset temperature for the exothermic reaction suggests that the reaction mechanism and respective rate-limiting processes might be different for ARM-prepared materials.

Focusing on low temperature processes, in this work the heat release during reaction in ARM material 2Al+3CuO in isothermal conditions was studied using a microcalorimeter TAM III by TA Instruments. Experiments with 2 Al+3CuO in TAM were conducted at three different temperatures: 303 K, 323 K, and 373 K. The samples used in the experiments differed by the aging time and conditions prior to the experiments. All samples were prepared by milling in Ar atmosphere using hexane as a process control agent (the general procedure is described in detail elsewhere [14]), and dried immediately after preparation for about 18 hrs in Ar atmosphere. After that, the storage conditions varied for different samples. Table 1 summarizes the conditions at which the material was stored before microcalorimetry measurements using TAM III.

Figure 2 shows the results of TAM III measurements in terms of both integral heat release and heat release rate, normalized by sample mass. All samples were exposed to the furnace temperature at the time equal to 0 s; however, the measurements are unavailable for the initial period of time while the sample is thermally equilibrating. The traces are shown after the TAM III signal became meaningful. The curves are grouped by the temperature at which the TAM III measurements were performed. Each curve within a group belonging to the same temperature corresponds to the sample with different pre-treatment history. Note that only one curve is shown for experiment performed at 303 K, corresponding to the freshly prepared sample. For that sample, a noticeable heat release is measured even at this relatively low temperature. Samples stored for a year after preparation did not exhibit any reaction when treated at 303 K.

The curves are seen to group based on the processing temperature, indicating that the processing temperature had the major effect on the reaction rate, while the pre-heating history resulted in measurable, but smaller effects.

Some difference between the measured reaction rates was observed for samples B and D with different storage conditions that were processed at 323 K with the sample D stored in Ar showing a slightly greater heat release. Reaction rates were effectively identical for the samples B and C that were stored at the same conditions, in air. Taking into account that these samples were from different batches of powder, this suggests good reproducibility of the TAM III measurements. Difference for the curves of the sample processed at 373 K is due to preprocessing of one of them (E) at 323 K, and its reaction at 373 K is slower than that of the sample F kept in air at room temperature.

Table 1. Aging/storage conditions for sample used in TAM studies

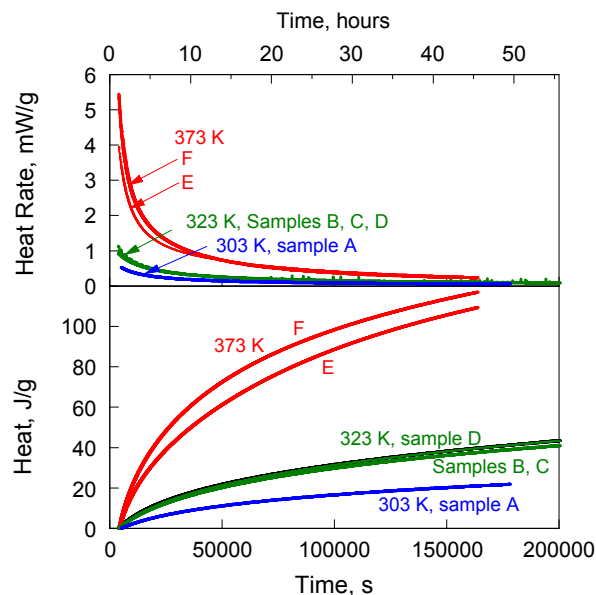| Sample ID	Temperature, K	Aging Conditions
A	303	Used immediately after drying
B	323	Stored for 1 day in air at room temperature
C	323	Stored for 1 day in air at room temperature
D	323	Stored for 1 day in Ar at room temperature
E	373	Stored for 1 day in air at room temperature; Exposed to 323 K for ~2.5 d
F	373	Stored for 5 days in air at room temperature

Fig. 2. Heat and rate of heat of reaction of 2Al+3CuO ARM nanocomposites at various temperatures obtained by microcalorimeter measurements.

Processing of the microcalorimetry and differential scanning calorimetry measurements

Differential scanning calorimetry (DSC) and TAM III data (microcalorimetry) provide quantitative measures of the heat flow generated in the sample upon its heating (DSC) or in isothermal conditions (microcalorimetry). This heat flow is used to estimate the extent of the redox reaction that should occur to account for the measured heat release. Alternatively, the values of heat flow can be translated into equivalent oxide layer thicknesses that should be grown as a result of the redox reactions. As described below, both measured heat flows and inferred values for the oxide thickness can be compared to those predicted theoretically considering different reaction mechanisms. Using this approach, the mechanism of the initial exothermic reaction can be elucidated.

The estimates for the growing oxide layer thickness were performed for the experimental data described above for microcalorimetry measurements and for data reported in ref. [14] for DSC measurements.

The predicted thickness of the oxide grown is a function of the assumed sample geometry. Two geometries are considered. In the spherical geometry, a spherical oxide inclusion is surrounded by Al matrix. In the planar geometry, layers of oxide and Al are placed on top of each other.

Figure 3 shows the oxide thickness estimated from the DSC measurements [14] for both geometries and assuming that 100 nm is the initial inclusion diameter and oxide layer thickness for the spherical and planar geometries, respectively. Note that for the spherical geometry, the result of the estimate also depends on the thickness of the initial oxide layer assumed to be present on surface of aluminum particle. This dependence is relatively as long as the thicknesses of oxide layers are small compared to the particle diameter. For consistency, several initial values for the initial alumina thickness were considered for both geometries.

It is interesting that a much greater oxide layer should be growing on the flat surface (about 6 nm) as compared to spherical particles (only about 1.5 nm) to explain the heat effect measured upon heating the nanocomposite sample in DSC furnace to 600 K.

Examples of similar estimates based on the microcalorimetry measurements are shown in Fig. 4. As in Fig. 3, the calculations are performed for both spherical and planar sample geometries. In this case, the thickness of the initial alumina layer is kept constant (0.5 nm) and the diameter of the inclusion or layer thickness are varied from 100 to 1000 nm for both geometries. As for the DSC measurements, a much thicker alumina layer is predicted to grow for the flat geometry than for spherical inclusions to explain the measured heat release.

Formulation of a theoretical reaction model

The results of TAM III measurements were interpreted using two reaction models. One of the models was conventional thermally activated diffusion [18], and the other was so-called Mott-Cabrera model developed to describe growth of initial thin oxide layers at low temperatures [19, 20]. In the latter model, the mass transfer rates are accelerated by electrostatic interaction of the diffusing ions and static electric charges developed principally due to the difference in mobility between ions and electrons. Because the focus of the present effort was to describe the onset of the heterogeneous exothermic reactions, the oxidation results in the growth of the initial, amorphous alumina layer. The polymorphic phase changes in alumina occur at higher temperatures and/or substantial oxide thicknesses [5 – 7] and thus play only secondary role for the processes of interest in this study. Transport (diffusion) of oxygen from the oxide core to aluminum matrix through a growing layer of alumina was considered as the reaction rate-limiting process. Note that this analysis is effectively equivalent to a case of aluminum ions diffusing to oxidizer; in the present simplified analysis, the nature of the diffusing species is not affecting the model outcome.

Because reactions of reduction of the metal oxidizers used in thermite systems may not occur in one step, each reaction model should represent a specific oxidizer. No change in the general model layout is required to modify it for a different oxidizer; however, specific reaction steps, products, and subproducts should be altered. As a first step the model formulated in this study considers an Al-CuO thermite. This material system is selected because of two primary reasons:

a. There is only one known intermediate copper oxide, Cu_2O that can be formed upon initial reduction of CuO before metallic copper is produced. For most of the other oxides used in practically interesting thermite compositions, more intermediate oxides can be formed resulting in a greater number of the anticipated reaction steps.

b. The cross-sectioned Al-CuO composites show good contrast in the SEM images and thus a relatively straightforward measurement of the sizes of Al and CuO domains present in the actual samples is possible, as needed for calibration and validation of the proposed model.

Schematically, the reactant configurations used in the model are illustrated in Fig. 3. For a spherical geometry, an inclusion of CuO is considered to be embedded into an Al matrix. For a planar geometry, flat layers or CuO and Al are placed on top of each other. For all cases, the reacting components, Al and CuO, are assumed to be initially separated by an amorphous alumina layer, similar to that present on surface of any aluminum particle exposed to air. This oxide layer can transform into

different alumina polymorphs at elevated temperatures and increased thickness [5 – 7].

It is assumed that the rate of oxygen diffusion within the oxide core is significantly higher than the rate of oxygen (or aluminum) diffusion through a growing layer of alumina. Therefore, the concentration of oxygen inside the oxide inclusion is always spatially uniform. In general case, the model considers two possible mechanisms: reduction steps for CuO through formation of Cu_2O and Cu, and reduction of CuO directly to Cu. According to the Cu-O phase diagram [21], at low temperatures (< 375 ºC) used in the microcalorimetry experiments, only CuO and Cu are stable in the binary Cu-O system.

In the case of conventional thermally activated diffusion, the growth of the alumina layer thickness, h, is described by the 'parabolic' law in case of planar geometry:

$$\frac{dh}{dt} = D_{O^-}\frac{C_{O^-}}{h} \tag{1}$$

where dh/dt is the rate of growth of the layer thickness, C_{O^-} is the oxygen ion concentration in oxide inclusion; and D_{O^-} is the diffusion coefficient for oxygen ions. For the spherical geometry, the equation takes form:

$$\frac{dh}{dt} = D_{O^-}\frac{C_{O^-}}{\dfrac{1}{r_{CuO}} - \dfrac{1}{r_{Al_2O_3}}}\frac{1}{r_{Al_2O_3}^{2}} \tag{2}$$

where r_{CuO} and $r_{Al_2O_3}$ are the radii of the oxide inclusion and alumina layer, respectively. The radii are changing as the oxidation continues, considering the amounts of the reacting species and respective densities of Al, CuO/Cu_2O mixture, and Al_2O_3.

For the thermally activated diffusion, diffusion coefficient is described by an Arrhenius equation:

$$D_{O^-} = D\cdot\exp\left(-\frac{E}{RT}\right) \tag{3}$$

where R is the universal gas constant, T is temperature, and the pre-exponent D and activation energy, E, can be taken from the aluminum oxidation studies or treated as adjustable parameters of the model.

The concentration of the diffusing species (oxygen anions) at the interface of aluminum and the growing alumina layer was assumed to be zero. Two different approaches were considered to determine the oxygen concentration inside the oxide inclusion, C_{O^-}. In one approach, the concentration of the mobile oxygen anions was calculated as equal to the oxygen concentration in the gas in equilibrium with the mixed CuO/Cu_2O oxides at a specific temperature. These concentrations are calculated using the p-T-x Cu-O phase diagram [21]. This approach produces a very small oxygen concentration, resulting in very low overall diffusion rates. Another approach assumes that the entire oxygen concentration present in

the CuO/Cu_2O oxide mixture is available for diffusion and produces an upper limit for the possible concentration of oxygen anions. In this latter case, the calculation begins with the concentration of oxygen in pure CuO and continues to adjust the oxygen concentration as the redox reaction removes oxygen from the copper oxides and transfers it to alumina.

An alternative reaction description for aluminum oxidation is given by Mott-Cabrera model [19, 20], considering formation of the initial, very thin, oxide coverage on the fresh aluminum surface. In this model, the diffusion is substantially assisted by electric fields formed due to the difference in the mobility of oxygen ions and electrons from the metal through the growing oxide layer. Electrons from metal diffuse through the oxide layer to the oxidizer side and assist in the formation of oxygen anions. Production of such anions assists in diffusion of metal cations through the growing oxide and their reaction with the oxygen anions. This reaction is much faster than conventional diffusion and results in a rapid growth of an initial oxide layer. The reaction slows down at a specific limiting thickness of the oxide film, with further oxidation governed by regular diffusion. The Mott-Cabrera electric field-assisted oxidation model leads to the following equation for the growth rate of the oxide thickness h [19, 20]:

$$\frac{dh}{dt} = \Omega n\nu\exp\left(\frac{-U + qaE_{M-C}}{k_B T}\right) \tag{4}$$

where k_B is the Boltzmann constant, U is the rate - limiting energy barrier, q is the charge of migrating cations, a is the distance between the positions of the potential well and barrier, Ω is the volume of oxide formed per one cation, ν is the attempt frequency of the cation jump, n is the number of cations per unit area that may jump through the energy barrier U. E_{M-C} is the electric field generated in the oxide film that assists aluminum cations to overcome the potential barrier. The electric field for the plane geometry is given by:
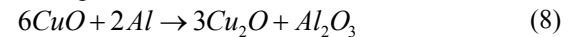
$$E = -\frac{V}{h} \tag{5}$$

For the spherical geometry, electric field is calculated as:

$$E = -\frac{Vr_{CuO}}{r_{Al_2O_3}h} \tag{6}$$

The chemical reactions considered to evaluate the reaction enthalpy compare the theoretical models with the DSC and microcalorimetry experiments are

$$3CuO + 2Al \rightarrow 3Cu + Al_2O_3 \tag{7}$$
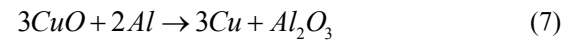
at temperatures < 375 ºC, and

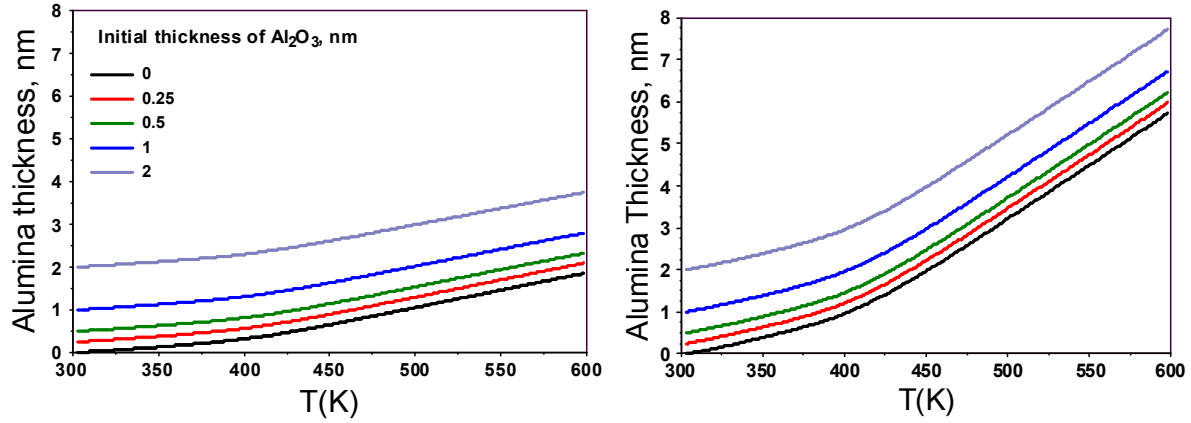$$6CuO + 2Al \rightarrow 3Cu_2O + Al_2O_3 \tag{8}$$

at higher temperatures.

Fig. 3. Thickness of the alumina oxide layer predicted to grow on the surface of a 100-nm CuO inclusion in DSC experiments [14] considering a spherical inclusion (left), and a flat layer (right).
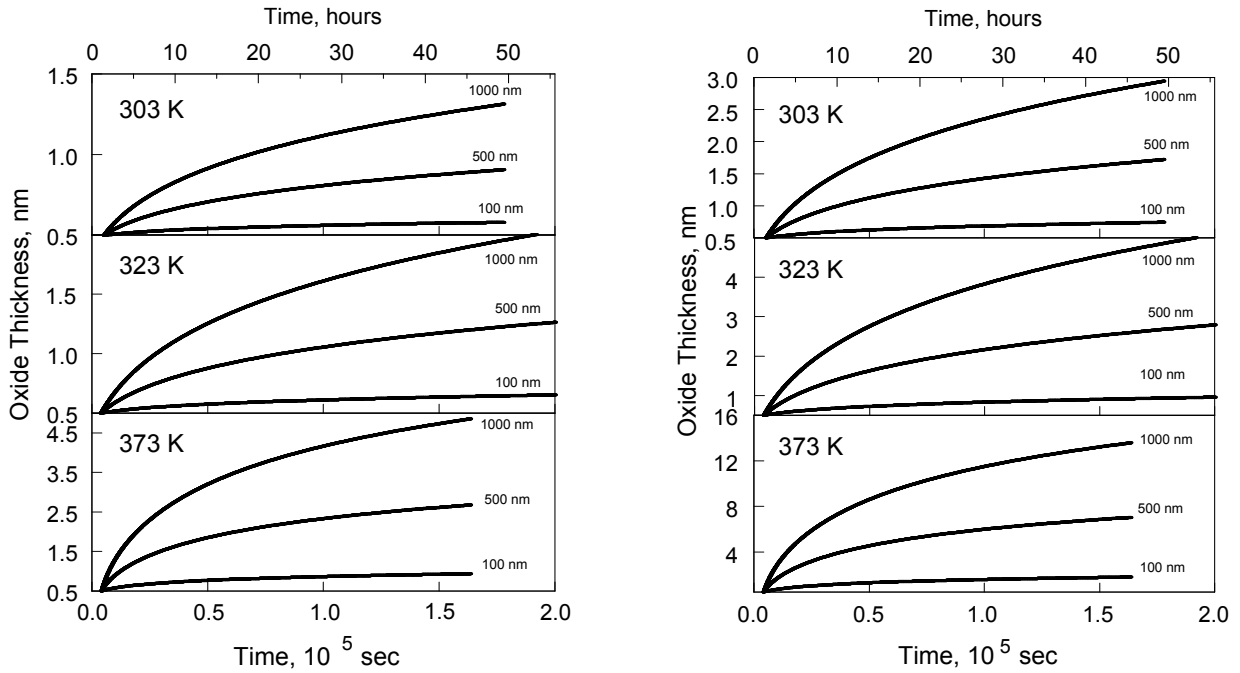

Fig. 4. Thickness of the alumina oxide layer estimated to grow in TAM III experiments at different temperatures. The calculations are performed for spherical inclusions (left) and flat layers (right) with the dimensions varied from 100 to 1000 nm. The initial oxide layer is assumed to be 0.5 nm for all cases.

Model predictions and their implications

Specific predictions of the oxidation rates based on a conventional thermally activated diffusion model used the reaction parameters identified in ref. [7] for the first detected step of oxidation of aluminum powders in thermogravimetric experiments. In ref. [5 – 7], the oxidation was actually detected at higher temperatures than in the experiments involving reactive nanocomposite materials (refs. [14 – 17] and present TAM III measurements), so that the Arrhenius term introduced in ref. [7] was extrapolated to describe reaction at lower temperature. As mentioned above, the concentration of oxygen available for diffusion was taken to be equal to that in the condensed CuO. This oxygen concentration is substantially higher than that available in experiments described in refs. [5 – 7] resulting in a significant increase in the oxidation rate.

For processing DSC experiments presented in ref. [14], the measured heat flows were directly compared to those predicted using the conventional thermally activated diffusion model. Results of this comparison are shown in Fig. 6. The bottom plots show measured and calculated heat flows and the top plots show oxide thickness estimated to be required to describe the experimental data. Note that separate thicknesses for the initially growing amorphous oxide and for the γ-Al_2O_3 polymorph formed later on are shown, as calculated in the oxidation model.

The shape of the experimental DSC curves could not be reproduced despite treating both activation energy and pre-exponent in the oxidation model as adjustable parameters. Even assuming the maximum possible concentration of oxygen inside the CuO inclusion or assuming an unrealistically high pre-exponential factor and/or unrealistically low activation energy resulted in an under-predicted reaction rate at low temperatures, at which the onset of the exothermic reaction was detected experimentally. When adjustable parameters were selected in unrealistic ranges, to predict at least some reaction at low temperatures, the predicted reaction, while starting late, occurred at the rates much higher than experimentally observed, indicating the critical deficiency of the diffusion-based oxidation model.

It is also interesting that the predicted evolution of the oxide layer is qualitatively different from that presented in Fig. 3, for which the same experimental results were processed without considering any specific oxidation model.

In summary, it appears to be impossible to match the measured DSC traces using the thermally activated diffusion model.

For the isothermal heating (TAM III experiment), the results of experiments are compared to the model predictions in terms of the rate of oxide growth. The rates of oxide growth for the results presented in Fig. 4 are shown in Fig. 7 as solid lines. Only results for samples A, B, and F are presented to simplify the discussion. As noted above, the temperature of the furnace affected the rate of oxidation most substantially, with only minor differences caused by the pre-heating and storage history.

Long-dashed lines in Fig. 7 show the oxide growth rates predicted using a thermally activated diffusion model. These rates are substantially lower than experimental, despite using the very high concentration of oxygen ions in CuO, as described above. Because the presented computed oxidation rates are very low, effectively no measurable growth occurs over the time of experiment and the changes in the oxidation rate are too small to be noticeable in Fig. 7. Again, this behavior is qualitatively different from that observed experimentally. The oxide growth rates computed using the Mott-Cabrera model are shown in Fig. 7 as short-dashed lines. All parameters describing the model were taken from ref. [22] and are suitable for oxidation of fresh Al surface in gaseous oxidizer. It is likely that these parameters need to be adjusted for the interface growing between aluminum and metal oxide. It is interesting that the discrepancy between the predicted and experimental data is much less than for the diffusion model. Most importantly, the Mott-Cabrera model predicts the change in the oxide growth rate that is qualitatively similar to that observed in experiments. It has been observed that considering some of the oxidation model parameters as adjustable, the experimental data can be matched with high accuracy. This was not possible with any choice of adjustable parameters for the simple diffusion model. Therefore, it is concluded that the oxidation reaction in nanocomposite thermites is initially well described by the Mott-Cabrera model, so that the transport of the reacting ions is assisted by electric field formed across the growing alumina layer.

Conclusions

New microcalorimetry experiments as well as analysis of the previously reported DSC measurements show that the onset of exothermic reaction in nanocomposite materials prepared by ARM occurs at substantially lower temperatures than in other Al-based composite and nano-composite materials. The analysis of the experimental data showed that a simple model of thermally activated diffusion cannot adequately describe the onset of oxidation in nanocomposite materials prepared by ARM. An alternative reaction description for aluminum oxidation is given by Mott-Cabrera model [19, 20], considering formation of the initial, very thin, oxide coverage on the fresh aluminum surface. In this model, the diffusion is substantially assisted by electric fields formed due to the difference in the mobility of oxygen ions and electrons from the metal through the growing oxide layer. Electrons from metal diffuse through the oxide layer to the oxidizer side and assist in the formation of oxygen anions. Production of such anions assists in diffusion of metal cations through the growing oxide and their reaction with the oxygen anions. This reaction is
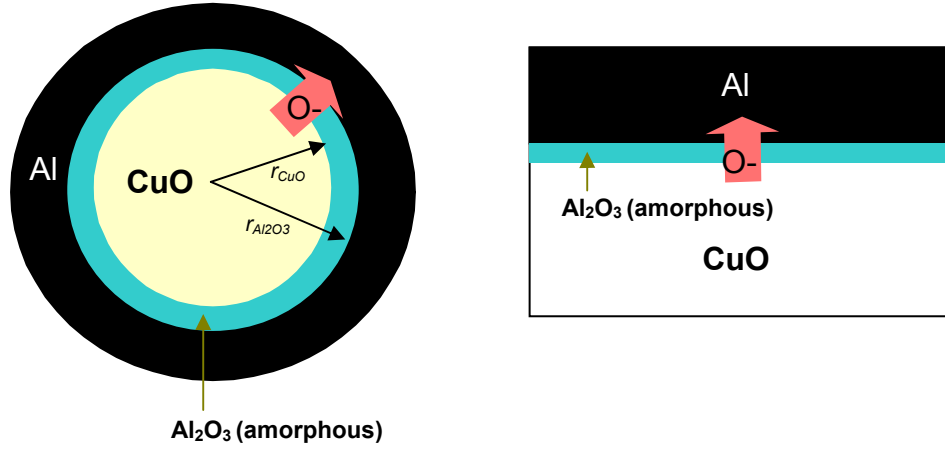
Fig. 5. Schematic diagram of reaction geometries considered in the models: a single spherical inclusion of oxidizer in an aluminum matrix (left) and planar layers (right).
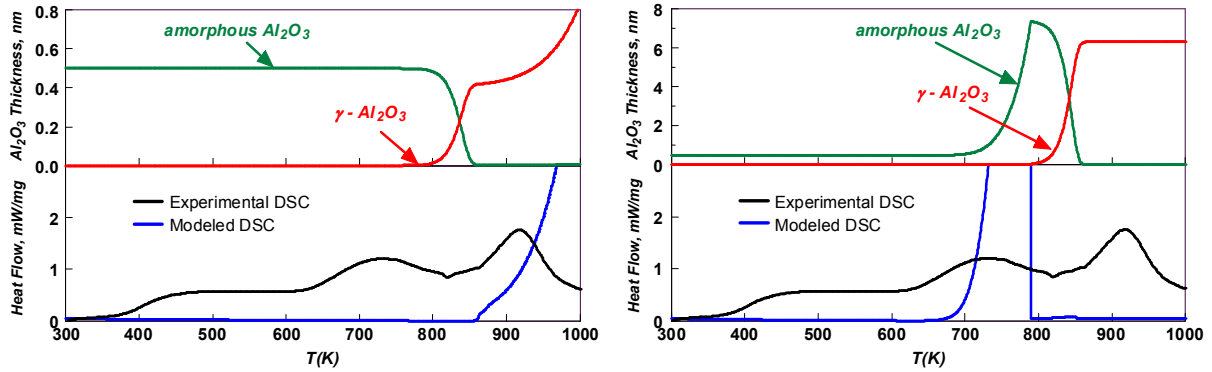

Fig. 6. Bottom plots: experimental DSC trace (black) [14] compared to the calculated heat flow traces using the developed model. The top plots show evolution of the amorphous oxide layer and its transformation into γ-Al$_2$O$_3$. The left plots show a calculation with realistic diffusion coefficient. The right plot shows a calculation with unrealistically high pre-exponent for the diffusion coefficient selected to shift the reaction onset to a lower temperature.
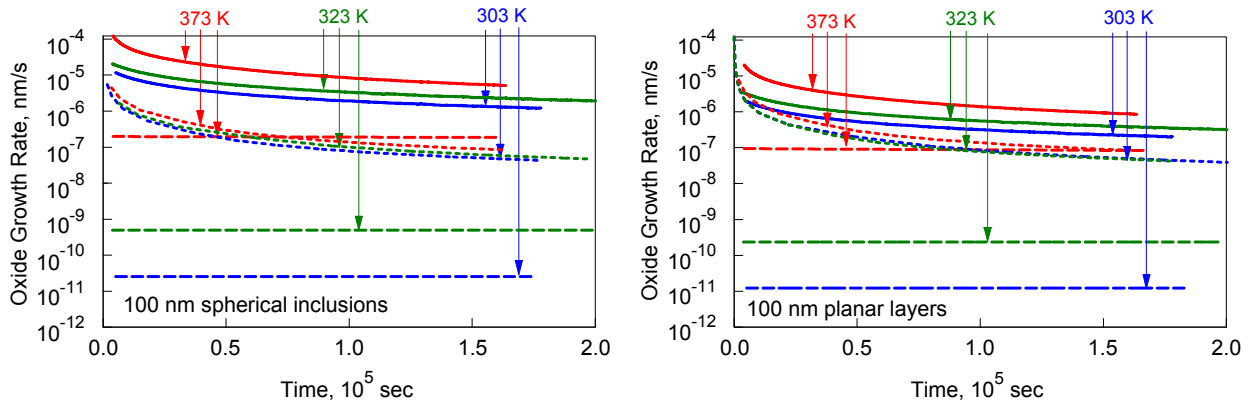

Fig. 7. Rates of Al oxide growth estimated from experimental microcalorimery data (solid lines) and their comparison with the theoretical predictions using thermally activated diffusion model (long dash) and Mott-Cabrera model (short dash) for spherical and planar geometries. Initial Al$_2$O$_3$ layer is assumed to be 0.5 nm thick for all cases.

faster than conventional diffusion and results in a rapid oxide growth at low temperatures. The reaction slows down at a specific limiting thickness of the oxide film, with further oxidation governed by regular diffusion. Preliminary estimates suggest that both the experimental DSC curves and microcalorimetry measurements can indeed be quantitatively described using the Mott-Cabrera reaction model.

Acknowledgement

References

[1] A. Dokhan, E.W. Price, J.M. Seitzman, R.K. Sigman, Proc. Combust. Inst. 29 (2002) 2939-2945.

[2] Q.S.M. Kwok, R.C. Fouchard, A.M. Turcotte,P.D. Lightfoot,R. Bowes, D.E.G. Jones, Propellants, Explos., Pyrotech. 27 (2002) 229-240.

[3] P. Brousseau, C.J. Anderson, Propellants, Explos., Pyrotech. 27 (2002) 300-306.

[4] M.A. Trunov, M. Schoenitz, E.L. Dreizin, Propellants, Explos., Pyrotech. 40 (2005) 36-43.

[5] M.A. Trunov, M. Schoenitz, X. Zhu, E.L. Dreizin, Combust. Flame 140 (2005) 310-318.

[6] M.A. Trunov, S.M. Umbrajkar,M. Schoenitz,J.T. Mang, E.L. Dreizin, J. Phys. Chem. B 110 (2006) 13094-13099.

[7] M.A. Trunov, M. Schoenitz, E.L. Dreizin, Combust. Theory Modell. 10 (2006) 603-624.

[8] E.L. Dreizin, M. Schoenitz, US Patent 7,524,355 B2 (2009).

[9] J. Sun,M.L. Pantoya, S.L. Simon, Thermochim. Acta 444 (2006) 117-127.

[10] R.-H. Fan, L. Hong-Liang, K.-N. Sun, W.-X. Wang, X.-B. Yi, Thermochim. Acta 440 (2006) 129–131.

[11] K.S. Martirosyan , L. Wang, D. Luss, Chem. Phys. Lett. 483 (2009) 107–110.

[12] K.J. Blobaum, A.J. Wagner, J.M. Plitzko, D. Van Heerden, D.H. Fairbrother, T.P. Weihs, J. Appl. Phys. 94 (2003) 2923-2929.

[13] K.J. Blobaum, M.E. Reiss, J.M. Plitzko Lawrence, T.P. Weihs, J. Appl. Phys. 94 (2003) 2915-2922.

[14] S.M. Umbrajkar, M. Schoenitz, E.L. Dreizin, Thermochim. Acta 451(2006) 34-43.

[15] M. Schoenitz, S. Umbrajkar E.L. Dreizin J. Prop. Power 23 (2007) 683 – 687.

[16] S.M. Umbrajkar, S. Seshadri, M. Schoenitz, V.K. Hoffmann, E.L. Dreizin J. Prop. Power 24 (2008) 192 – 198.

[17] S.M. Umbrajkar, C.M. Chen, M. Schoenitz, E.L. Dreizin Thermochim. Acta 477 (2008) 1 – 6.

[18] O. Kubaschewski, B.E. Hopkins, Oxidation of Metals and Alloys, Butterworths, London, U.K., 1962.

[19] N. Cabrera, N.F. Mott, Rep. Prog. Phys. 12 (1949) 163-184.

[20] V.P. Zhdanov, B. Kasemo, Chem. Phys. Lett. 452(2008) 285 – 288.

[21] Y.V. Levinsky, P-t-x Handbook, Pressure Dependent Phase Diagrams of Binary Alloys, ASM International, Materials Park, OH, Stuttgart, Germany, 1997.

[22] L.P.H. Jeurgens, W.G. Sloof, F.D. Tichelaar, E.J. Mittemeijer, J. Appl. Phys. 92 (2002) 1649 – 1656.